

## Modelling of capillary coatings and heat exchange surfaces of elements of thermal power plants

A. A. Genbach<sup>1</sup>, D. Yu. Bondartsev<sup>1</sup>, I. K. Iliev<sup>2\*</sup>

<sup>1</sup>Almaty University of Power Engineering and Telecommunications, Department of Heat Engineering Installations, 126, A. Baitursynov Str., 050013 Almaty, Kazakhstan

<sup>2</sup>University of Ruse, Department of Thermotechnics, Hydraulics and Ecology, 8 Studentska Str., 7017, Ruse, Bulgaria

Modelling of the capillary porous structures and similarity of their processes allow to reveal a mechanism of heat transfer during steam generation of liquids, as well as determine zones of rising and developing fatigue cracks in the activation centres of steam seeds, research natural saline deposits and scale deposits and artificial porous coatings applicable on the metal fencing (plates) up to occurrence of the material limit state. Coatings are made of weak heat conductive mineral environment (quartz, granite, teshenite) with low porosity (3÷30%). Heat was initiated from flare of the jet burner and electric current. Stability of heat transfer was maintained by excessive cooler under joint action of capillary and mass forces. Solution related to the thermo elasticity resulted in relation of heat flows, heat stresses and destructive energy from time of heat supply and size of torn particles of coating. The areas of relaxation, breakup micro and macro processes were determined that demonstrate causes of rising and developing fatigue cracks of the heat and power equipment in stress concentrator with further development of erosion processes and relations of limit states of compression and tension to unity. The performed research took place for boiler-and-turbine load switching operations, as well as for establishing capillary porous cooling systems.

**Keywords:** Porous foam generator, foam generation, foaming, defoaming, heat-mass exchange, capillary-porous structures.

### INTRODUCTION

Studies of a porous cooling system for rocket type burners [1,4] was the result of burners development [2,3]. When a mineral weak heat-conducting porous coating is exposed to the thermal action of a burner, after a while a part of the surface heats up to a certain temperature, and other parts of the coating keep the initial temperature. Therefore, a temperature gradient develops inside the porous coating resulted in unequal expansion. The surrounding unheated layers exhibit resistance to this expansion. As a result, thermal stresses occur both in the heated part and in the surrounding unheated part, including the base layer. These stresses can acquire destructive values. The thermoelastic stress problem solutions for idealized processes are given in sources [4]. Normal compressive stresses played the dominant role in destruction process. Porous coating is subjected to destruction as a result of lost stability in a thin layer adjacent to free surface. Therefore, primary focus was on the stressed state of the upper layer, which

thickness depends on heat transfer coefficient and structure of coating and base layer (the metal steam-generating surface).

The vacancy density rapidly increases in the irradiated coating; these vacancies quickly combine with cavity pockets formation due to the fact that the vacancy combining process intensity is proportional to their density square. If the vacancy cavities can transform into dislocations, the irradiated coating acquires plastic properties and does not undergo a destruction process when affected by a burner. This is typical for all metals. Several mineral rocks (tuff, marble, limestone) have the same property.

If no dislocations form in the coating, the growing vacancy cavities concentrate stress at their edges and lead to destruction while the coating thermal stresses are still below the plastic yield point. There is brittle thermal destruction.

As described in the literature, illusory contradictions occur in course of developing a mechanism of the heat exchange process in porous structures for cooling-off the heat exchange surfaces of the power plant elements up to the critical heat fluxes ( $\sim 10^6$  W/m<sup>2</sup>), which happens when the wall medium type - liquid, steam or steam and water mixture - is under discussion. Our works show that

\* To whom all correspondence should be sent:  
iliev@enconservices.com

all the models do not contradict each other, but describe different boiling regimes [1].

Previously, using the methods of photoelasticity and holography, the destruction mechanism of the porous cooling system of the fire-jet burners' combustion chambers and nozzles was investigated [4]. It is interesting to compare the intensity of heat transfer [5–7] and the surface limit state [8, 9, 12], as well as to evaluate possible mechanisms for the destruction of heating (cooling) surfaces covered with capillary-porous structures [4]. This is in relation to the tasks of increasing the capacity of the thermal power equipment of power plants [10,11]. Such a problem is long overdue in connection with the modernization and extension of the life of gas turbine power plants.

### PHYSICAL MODEL OF THE HEAT AND MASS TRANSFER PROCESS

Dynamic models of heat transfer intensification during boiling on porous surface are generated based on experimental and theoretical studies. Developed surfaces contain interconnected internal cavities in the form of rectangular channels and small pores that connect the channels with the liquid pool.

The ratio of latent heat flux ( $\frac{\pi}{6} \bar{D}_d^3 \rho_s \bar{n} \bar{f}$ ) to the total heat flux for a developed surface can be (2...5) times more than that for an ordinary surface with a specific heat flux up to  $1 \times 10^4$  W/m<sup>2</sup>. That ratio decreased at high heat fluxes. Some data showed deviation of 300% from the calculated ones.

The formula includes the following legend:  $\bar{D}_d$  – average steam bubble departure diameter in a porous structure;  $r$  – specific evaporation heat;  $\rho_s$  – steam density;  $\bar{n}$  – average nucleation center density;  $\bar{f}$  – average steam bubble generation frequency.

Let us develop a physical model for transferring the specific heat flux “q” through the steam-generating surface (a wall or a base layer) covered with a capillary-porous structure (Fig.1).

The heat and mass transfer processes in the porous coating produce excessive liquid  $\tilde{m} = m_l/m_s$  due to the pressure potential activity generated by the capillary and mass forces  $\Delta P_{cap+g}$ .

The investigated thermal and hydraulic (internal) boiling characteristics [4] allow to show mechanism, to describe nature of the heat and mass transfer process in the investigated mesh porous structures [1,3] exposed to the gravitational force field, and

derive calculated equations for determining the diverted heat flux [3].

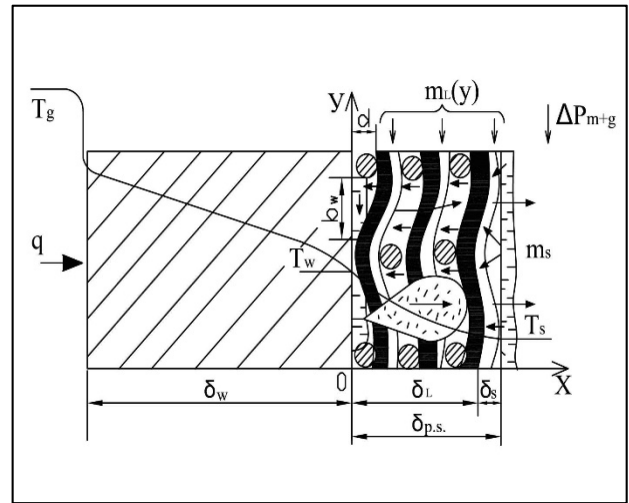


**Fig.1.** Physical model of the heat and mass transfer process in a real porous coating structure exposed to excessive liquid

The heat in the cooling system under study is transferred at small heat fluxes due to convective heat exchange with the value as higher as greater the effective thermal conductivity of the structure wetted with liquid and the housing thermal conductivity become. The fluid flow is smooth, and no steam bubbles or associated perturbing processes can be observed on the liquid surface. The liquid evaporates intensely from the menisci at low coolant excess; evaporation from the flowing film surface begins with an excessive liquid increase [3].

A certain heat flux, as smaller as lower  $\tilde{m} = m_l/m_s$  parameter becomes, causes disturbance of the smooth wavy flow liquid film producing single steam bubbles. Several actively-operating structure meshes represent permanent generation centers. Liquid boiling start  $\Delta T_{b.s.}$  depends on many regime and design parameters and can be determined with the equation aimed for this process,  $\Delta T_{b.s.}$ , which corresponds to the heat flux  $q_{b.s.}$  Reduction in the cooling liquid flow rate  $m_{l(s)}$ , or increase in the heat influx  $q$  cause a rapid growth of the evaporation centers.

Each center in the initial boiling regime works with unequal intensity, some heating surface areas are barely affected by the awakening centers which start working. If the circulating coolant rate  $m_{l(s)}$  increases, the lifetime of individual steam bubbles increases, and a number of active pores cease operation, long pauses occur between the bubble

nucleation moments, up to excluding such a center from a group of actively-generating ones. Excessive liquid increase “ $\tilde{m}$ ” makes other active generation centers inactive and feeble.

The transition zone to developed bubble boiling is not large due to the high rate of the active steam generation center growth “ $\tilde{n}$ ”. Further growth of the heat load “ $q$ ” results in many steady-operating active bubble formation centers, their uniform distribution throughout the steam generating surface. However, certain critical conditions can lead to a boiling crisis and a burned-out surface. Therefore, the compared deliberate destruction processes applied to fragile materials and the boiling crisis allow to model them and identify mechanism adopted by such processes.

### EXPERIMENTAL RESULTS

The destruction process mechanism was studied through experiments which included photoelasticity and holography method application [2]. The model stress state at similar times was evaluated by photographic recording of isochromatic patterns and counting the n-bars order at different points in the studied directions.

The thermoelasticity problem solution makes it possible to determine the medium limit state for a porous coating and a metal steam generating surface [4]. In case weak heat-conducting semi-porous

coatings and a metal wall (a base layer) are subjected to the thermal destruction, it is required to determine the effect produced by the specific heat flux “ $q$ ” applied to the surface and the time of its influence “ $\tau$ ” on the destructive stress generation “ $\sigma$ ”, the husk grain size composition (the detached particle size), and for the metal is the temperature perturbation depth penetration “ $\delta$ ”.

As the “ $q$ ” value increases within a short period of time “ $\tau$ ”, the dynamic effects become very significant, the compressive stresses “ $\sigma$ ” reach large values, typically several times higher than the material compressive strength. Therefore, it is necessary to take into account these stresses in the material thermal destruction mechanism. We need to find out what “ $\sigma_i$ ” stress type reaches its limit values earlier.

Consider a plate  $2h$  in thickness. A constant specific heat flux “ $q$ ” is being applied to the surface  $z=+h$  starting from  $\tau=0$  timepoint. The plate bottom surface  $z=-h$  and lateral edges are thermally insulated.

The plate temperature distribution value makes it possible to calculate the thermal stresses of tension and compression arising at a certain timepoint “ $\tau$ ” at different depths measured out from the surface  $\delta_i$  ( $h=z_i$ ) at a given heat flux “ $q$ ”, since the plate with a variable temperature over its thickness is plane-stressed [4].

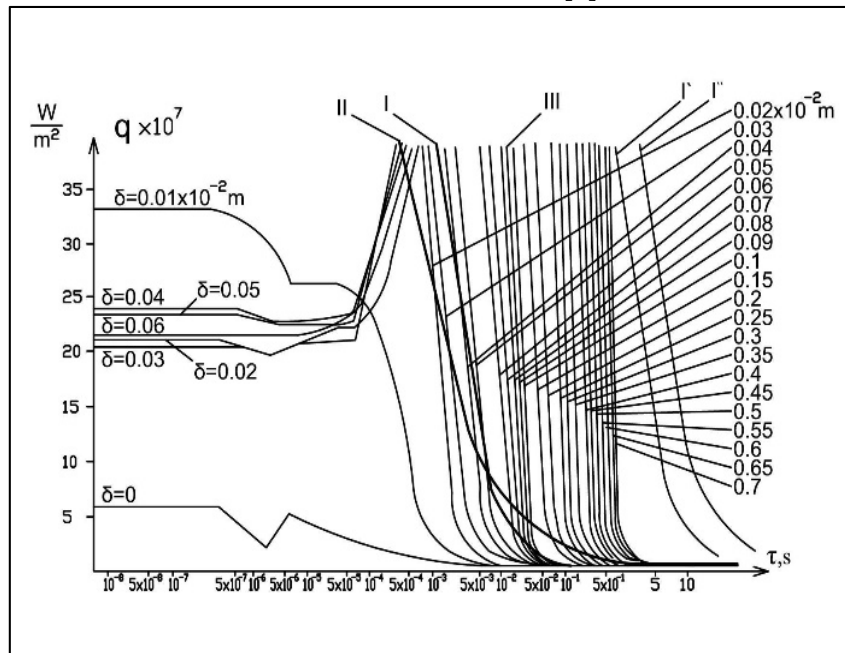


**Fig.2.** Dependence of heat fluxes “ $q_i$ ” causing the compressive stresses III of the quartz coating in relation to the time “ $\tau$ ” for different detached particle thickness “ $\delta_i$ ”: I – tensile stresses sufficient for destruction; I’, I’’ – copper and stainless steel,  $h = 0,1 \cdot 10^{-3}$  m; II – surface fusion

Assume the limit stress values of the compression  $\sigma_{lim.compr.}$  and tension  $\sigma_{lim.tens.}$  for the coating and metal, this will show us the functional dependence of the heat flux “q” required for the destruction on the delivery time “ $\tau$ ” and the penetration depth “ $\delta$ ”. In addition, the plate surface temperatures equated to the melting temperature  $T_{pl.}$  appropriate for the coating and metal, clarify the specific heat flux values necessary for melting-down the surface layer for a specific period of their action “ $q_i$ ”, i.e. in each

specific case we can trace functional dependences of the heat flux on the time it influences the rock and metal surface [4].

When it comes to a quartz plate (coating), the heat fluxes “ $q_i$ ” have been calculated for a wide time interval of  $10^{-8} \dots 10^3$  s. The lower limit of this interval ( $10^{-8}$  s) is the relaxation time. Fig. 2 illustrates that the  $q_1$  and  $q_2$  value ratios for the time intervals  $10^{-8} \dots 10^3$  s lose their physical significance.

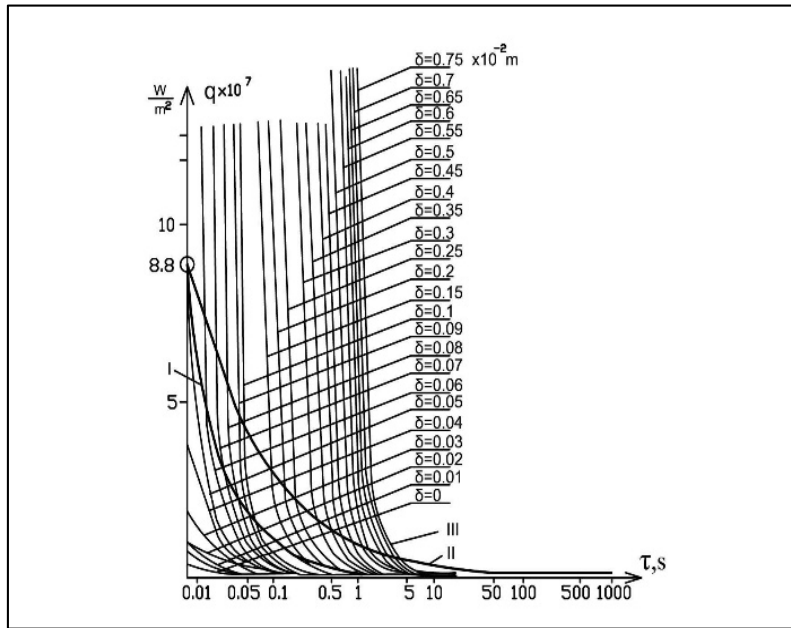


**Fig.3.** Dependence of heat fluxes “ $q_i$ ” causing the compressive stresses III of the quartz coating in relation to the time “ $\tau$ ” for different detached particle thickness  $\delta$ : I – tensile stresses sufficient for destruction; II – surface fusion; curves II<sup>1</sup> – copper,  $\delta = 0.1 \cdot 10^{-3}$  and II<sup>11</sup> – stainless steel,  $\delta = 0.1 \cdot 10^{-3}$  m, almost coincide with curve I in the region (0.01...0.1) s

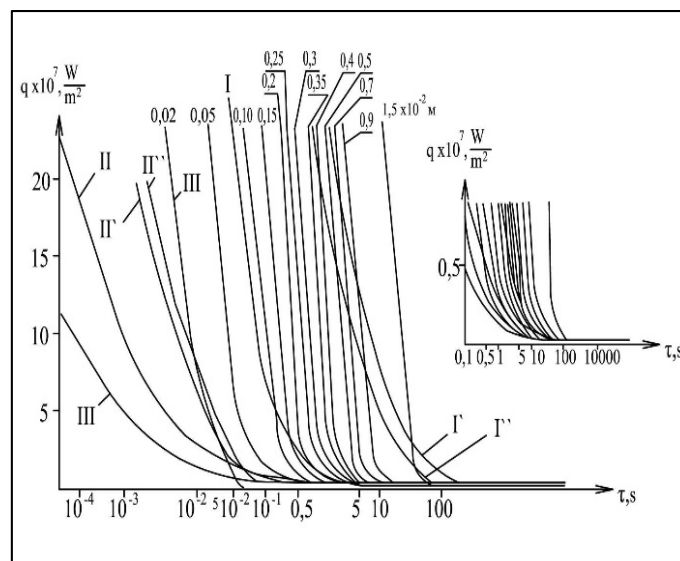


**Fig.4.** Dependence of heat fluxes “ $q_i$ ” causing the compressive stresses III of the granite coating in relation to the time “ $\tau$ ” for different detached particle thickness  $\delta$ : I – tensile stresses sufficient for destruction (I', I'' - copper and stainless steel,  $h = 0.1 \cdot 10^{-3}$  m); II – surface fusion (II', II'' - copper and stainless steel,  $h = 0.1 \cdot 10^{-3}$  m)

Since thermal destruction is a macro process, we consider that it lasts  $5 \cdot 10^{-3} \dots 10^3$  s. The coating destruction only by compression presents us a number of curves, corresponding to a specific detached particle thickness, which is  $(0.25 \dots 0.3) \cdot 10^{-2}$  m for teshenite, as evidenced experimentally through high-speed shooting with a SKS-1M camera.

The compression curve sections, which determine  $\delta > 0.3 \cdot 10^{-2}$  m thick particle detachment for the large values “q” and small values “ $\tau$ ”, are screened by the melting curve II, and by the tension curve I in the case of small heat fluxes and significant time intervals. The quartz coating surface melting curve is much higher than that of the teshenite coating, which explains its steady brittle destruction (Figs.2, 3).

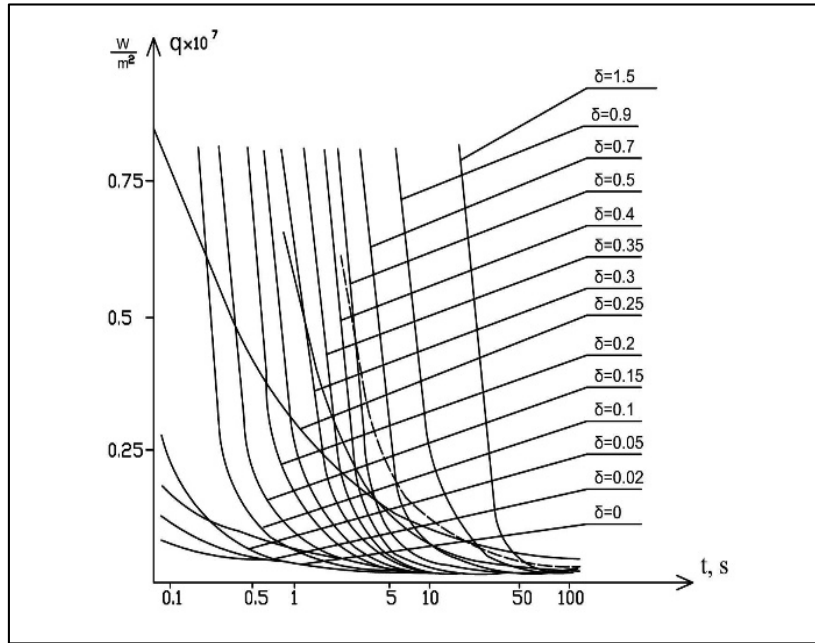


Fig.5. Dependence of  $q_i = f(\tau)$  shown in Fig.4 in the range of  $q = (0.25 \dots 0.75) \cdot 10^7$  W/m<sup>2</sup>

Boiler-and-turbine part destruction depends on the background of cracks in the stress concentrator (a relaxation zone) (see Fig.2). An explosive steam center formation (the time interval of  $10^{-8}$  s to  $10^{-3}$  s) represents a starting point for counting. The energy generated due to a steam bubble spontaneous appearance is close to the constant (invariant) value considering the time of its growth. It is spent on sustaining the center with a radius  $R_c$  and prevents its collapse ( $q$  values reach up to  $10^8$  W/m<sup>2</sup>). At this time, a thermodynamic equilibrium is under consideration for transition from a microprocess (microparticles and clusters with radii  $(10^{-7} \div 10^{-8})$  m (nano particles) of individual (single) bubbles to processes taking into account the behavior displayed by a large number of bubbles, i.e. with the help of integral characteristics ( $\bar{q}$ ,  $\bar{\alpha}$ ,  $\bar{\Delta T}$ ,  $\bar{\Delta P}$ ,  $\bar{w}$ ), where  $\bar{\alpha}$ ,  $\bar{\Delta T}$ ,  $\bar{\Delta P}$ ,  $\bar{w}$  is the average value of heat transfer coefficient, temperature and hydro-gas-dynamic head and flux velocity. The presence of stress concentrates, which generate an active steam phase,

significantly reduces the  $\sigma_{lim.compr.} / \sigma_{lim.tens.}$  ratio and this value can be of  $(1 \div 2)$ , in particular, for energy steels. It is also necessary to take into account presence of other stress concentrators, cyclicity produced by loads while the equipment operates in start/shutdown modes leading to fatigue cracks (stresses).

For example, the tensile strength for turbine steels is  $\sigma_b \approx (400 \div 1000)$  MPa. The yield point at operating temperature of  $-(400 \div 550)^\circ\text{C}$  decreases to  $(200 \div 900)$  MPa with deformation of 0,2%. The long-term strength limits decrease to  $(70 \div 260)$  MPa with deformation of  $(10 \div 20)\%$ . The temporary thermal stress value decreases to  $(40 \div 120)$  MPa, i.e. by an order of magnitude. The main estimated fatigue stresses amount only up to 0.45 of  $\sigma_b$ .

Therefore, the likelihood is great that the values  $\sigma_{lim.tens.} \approx \sigma_{lim.compr.}$ , and  $\sigma_{lim.tens.}$  values grow to 10 MPa and become of the same magnitude for porous coatings. The bubble “death” processes, as well as nucleation are also explosive ( $\tau = 10^{-8} \div 10^{-6}$  s) and

lead to the cumulative event appearance, which destroys the stress concentrator (an active generation center) by erosion along with corrosion and electrical processes and, as a result, its size reaches the critical crack point. In the case of instant steam condensation in a pit (a hole), the steam instantly disappears forming a powerful cumulative effect (cavitation), while shock waves are distributed deep into the parts and cracks develop admitting oxygen inside.

At the very moment a bubble or a drop are “born”,  $\alpha$  value is up to  $1 \cdot 10^5$  W/m<sup>2</sup>K at a steam temperature (500÷565)°C the  $\Delta T$  value reaches 500°C, and  $q$  value acting at the bubble bottom (the “dry” spot zone) is up to  $5 \cdot 10^7$  W/m<sup>2</sup>. Given that an individual steam bubble generates  $q$  value 10 times more than its integral value [1], then the total  $q$  value is  $5 \cdot 10^8$  W/m<sup>2</sup>, which is represented in the figures  $q=q(\tau, \delta)$ . The greater the heat wave penetration depth “ $\delta$ ” (or that of a particle detached from the porous coating), the longer it will take to destroy the parts (see Figs.2-6 for “ $q$ ”). The interrelation between compressive and tensile stresses is a stress diagram within the plate (coating) for various time intervals calculated from moment the process under consideration begins. At small  $\tau$  values,  $10^{-2}$  s magnitude, only compressive stresses occur. Starting from  $\tau = 10^{-1}$  s, in some region  $\Delta(h-z_i)$  the compressive stress turns into a tensile stress, and they are at different depths from the plate surface for different time intervals.

The destruction of the coating and metal subjected to compressive forces happens much earlier than that subjected to the tensile forces. The heat flux intervals, within which such destruction occurs, are as follows:  $q_{max}=7 \cdot 10^7$  W/m<sup>2</sup>,  $q_{min}=8 \cdot 10^4$  W/m<sup>2</sup> for quartz coatings,  $q_{max}=1 \cdot 10^7$  W/m<sup>2</sup>,  $q_{min}=21 \cdot 10^4$  W/m<sup>2</sup> for granite coating,  $q_{max}=2 \cdot 10^6$  W/m<sup>2</sup> for metal (a base layer) (boiling crisis in a porous system);  $q_{min}=1 \cdot 10^4$  W/m<sup>2</sup> (without cooling).

As  $q$  value increases in the heated layer, and therefore, the heating time “ $\tau$ ” decreases, the role played by compressive stress becomes more significant. Despite the high resistance to compression, destruction produced by compressive thermal stresses takes place in more favorable conditions instantly and in small volumes. Figs.2-6 displays curves for steam generating heating surfaces at the moment a film regime was established and the surface temperature increased

sharply to a value of  $T_{pl}$ . resulting from the boiling regime change. The calculated specific energy  $Q$  of a destructed volume unit of quartz, granite and teshenite coatings shows that the curves have expressed minimum values depending on the detached particle thickness “ $\delta$ ”.

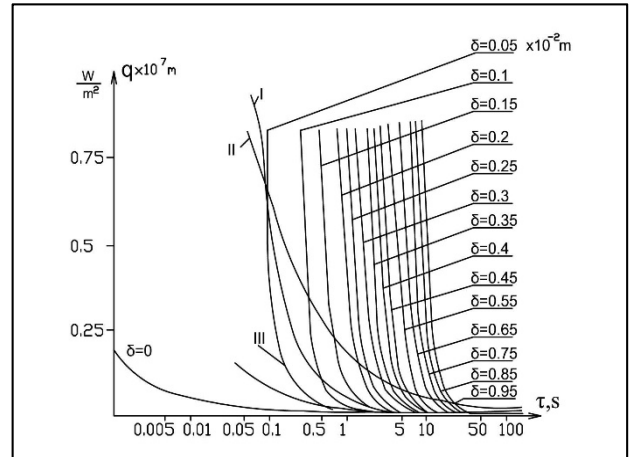


**Fig.6.** Dependence of heat fluxes “ $q_i$ ” causing the compressive stresses of the teshenite coating in relation to the time “ $\tau$ ” for different detached particle thickness  $\delta_i$ : I – tensile stresses sufficient for destruction; II – surface fusion; III – destructive compressive thermal stresses. Curves II и II’ for copper and steel almost coincide with curve I in the interval  $\tau = (0.1 \dots 1)$  s; metal thickness  $\delta_{pl} = h = 0.1 \cdot 10^{-3}$  m.

The minimum energy consumption for a quartz coating under destruction conditions is  $Q \cong 0.5 \cdot 10^3$  J/m<sup>3</sup>, where  $\tau=(0.1 \div 1)$  s,  $\delta_i=(0.1 \div 0.25) \cdot 10^{-2}$  m.

For granite coating:  $Q \cong 2.5 \cdot 10^9$  J/m<sup>3</sup>, where  $\tau=(0.1 \div 5)$  s,  $\delta_i=(0.1 \div 0.3) \cdot 10^{-2}$  m, where  $q \cong 0.1 \cdot 10^7$  W/m<sup>2</sup> and  $\delta=(0.2 \div 1.5) \cdot 10^{-2}$  m,  $Q=2.5 \cdot 10^9$  J/m<sup>3</sup>.

For teshenite coating:  $Q \cong 0.5 \cdot 10^9$  J/m<sup>3</sup>, where  $\tau=(0.1 \div 5)$  s,  $\delta_i=(0.1 \div 0.4) \cdot 10^{-2}$  m, provided that the ratio of the limit normal compressive and tensile stresses varied from 20 to 30.

## CONCLUSIONS

The microcrack presence in the monolith coating reduces its compressive strength in the crack area so that the compressive strength can be only 2 times greater than the tensile strength. The curves  $Q=f(q)$  shift their minimum values with grows “ $\delta_i$ ” toward decreasing “ $q$ ”, provided that a lower energy consumption “ $Q$ ” is required for the thermally destructed brittle coatings. Thus, the limit thermal stress generation is very likely at the start/shutdown of boiler-and-turbine equipment at power plants.

These stresses arise primarily in the concentrator areas, which are the nucleation centers for the active steam phase, or condensate drop formation. The capillary-porous structure can be of natural origin (salt deposits, film), and produced artificially with usage of well and weak heat-conducting materials over a wide porosity range from 3% to 90% (penetration). The structures can both be a model and act as a high-intensity and forced cooling system. For example, teshenite porous coatings with a linear expansion coefficient 5 times greater, thermal conductivity coefficient 10 times lower and approximately the same melting temperature compared to those of energy steels serve as a modeling material. They demonstrate the highest viscosity with a porosity of up to 30%.

#### NOMENCLATURE

$q$  – specific heat flux, W/m<sup>2</sup>;  
 $T_g, T_w, T_s$  – gas, wall (base layer) and saturation temperatures, °C;  
 $\delta_w, \delta_l, \delta_s, \delta_w$  – wall, liquid, steam, wick thickness, m;  
 $m_{l(s)}, m_s$  – liquid and steam flow, kg/s;  
 $\Delta P_{cap+g}$  – effective driving capillary and mass head, N/m<sup>2</sup>;  
 $d$  – grain size, m;  
 $b_w$  – porous material cell width, m.

#### Subscripts

$g$  – gas;  
 $w$  – wall;  
 $s$  – saturation;  
 $l$  – liquid;  
 $s$  – steam;  
 $w$  – wick thickness;  
 $cap+g$  – capillary and mass.

#### REFERENCES

- [1] Polyayev V.M., Genbach A.A., Control of Heat Transfer in a Porous Cooling System. Proceedings, 2<sup>nd</sup> World Conference on Experimental Heat Transfer, Fluid Mechanics and Thermodynamics, Dubrovnik, Yugoslavia, 639-644 (1991).  
 [2] Polyayev V.M., Genbach A.N., Genbach A.A. An experimental study of thermal stress in porous materials by methods of holography and photoelasticity // Experimental thermal and fluid science, avenue of the Americas, New York, volume 5, number 6, 697-702, November (1992).  
 [3] Polyayev V.M., Genbach A.A., Heat transfer in a porous system operating under the combined action of capillary and gravitational forces. (in Russian), // Thermal Engineering, 7, 55-58, (1993).  
 [4] Genbach A.A., Bondartsev D.Yu., Iliev I.K. Investigation of a high-forced cooling system for the

elements of heat power installations. Journal of Machine Engineering, 2018, Vol. 18, №2, 106-117. DOI: 10.5604/01.3001.0012.0937

[5] Shklover E.G. Experimental study of heat transfer from porous surface in pool and forced – convection boiling at low pressures // Phase Change Heat Transfer ASME. 1991. V. 159. P. 75-80. DOI: 10.1080/08916152.2017.1397821

[6] A.S. Surtaev, V.S. Serdyukov, A.N. Pavlenko, D.V. Kozlov, D.S. Selishchev. Characteristics of boiling heat transfer on hydrophilic surface with SiO<sub>2</sub> coating. *Bulgarian Chemical Communications, Vol. 50, Special Issue K (pp. 36 – 44) 2018*

[7] L.L. Tovazhnyansky, P.O. Kapustenko, O.A. Vasilenko, S.K. Kusakov, O.P. Arsenyeva, P.Y. Arsenyev. Mathematical model of a plate heat exchanger for condensation of steam in the presence of non-condensing gas. *Bulgarian Chemical Comm., Vol. 50, Special Issue K (pp. 76 – 82) 2018*

[8] Jamialahmadi M., Müller-Steinhagen H., Abdollahi H., Shariati A. Experimental and theoretical studies on subcooled flow boiling of pure liquids and multicomponent mixtures // Int. J. Heat and Mass Transfer. 2008. V. 51. P. 2482-2493. DOI: 10.1016/j.ijheatmasstransfer.2007.07.052

[9] Krepper E., Koncar B., Egorov Yu. CFD modelling of subcooled boiling - Concept, validation and application to fuel assembly design // Nuclear Engineering and Design. 2007. V. 7. P.716-731. DOI:10.1016/j.nucengdes.2006.10.023

[10] Kupetz M., Jeni Heiew E., Hiss F. Modernization and extension of the life of steam turbine power plants in Eastern Europe and Russia // Heat Power Engineering. 2014. V. 6. P. 35-43. DOI: 10.1134/S0040601514060056

[11] Grin E.A. The possibilities of fracture mechanics in relation to the problems of strength, resource and justification for the safe operation of thermal mechanical equipment // Heat Power Engineering. 2014. V. 1. P. 25-32.

[12] Z.Q. Yu, G.S. Zhou, S.D. Zhu, J.M. Li, L.J. Li. Influence of sensitizing treatment on the corrosion resistance of Incoloy 028 alloy. *Bulgarian Chemical Communications, Vol. 49, Number 4, (pp. 943 – 947) 2017.*